N93-32119

Graphics Simulation and Training Aids for Advanced Teleoperation

Won S. Kim, Paul S. Schenker, and Antal K. Bejczy

Jet Propulsion Laboratory
California Institute of Technology
4800 Oak Grove Drive
Pasadena, CA 91109

ABSTRACT

Graphics displays can be of significant aid in accomplishing a teleoperation task throughout all three phases of off-line task analysis and planning, operator training, and on-line operation. In the first phase, graphics displays provide substantial aid to investigate workcell layout, motion planning with collision detection and with possible redundancy resolution, and planning for camera views. In the second phase, graphics displays can serve as very useful tools for introductory training of operators before training them on actual hardware. In the third phase, graphics displays can be used for previewing planned motions and monitoring actual motions in any desired viewing angle, or, when communication time delay prevails, for providing predictive graphics overlay on the actual camera view of the remote site to show the non-time-delayed consequencies of commanded motions in real time. This paper addresses potential space applications of graphics displays in all three operational phases of advanced teleoperation. Possible applications are illustrated with techniques developed and demonstrated in the Advanced Teloperation laboratory at Jet Propulsion Laboratory. The examples described include task analysis and planning of a simulated Solar Maximum Satellite Repair task, a novel force-reflecting teleoperation simulator for operator training, and preview and predictive displays for on-line operations.

I. INTRODUCTION

Advances in computer graphics technologies enable the design, development, and use of high-fidelity graphics displays for very efficient operation aid in space telerobotics. Advanced graphics techniques [10] can be used to achieve increased reliability in all three phases of space telerobotic operations: in off-line task analysis and planning, in operator training, and in on-line task execution. This paper addresses potential use of graphics displays in all three phases of space telerobotics flight experiments. All three applications areas are described and illustrated by examples implemented at the Advanced Teleoperation Project [3], [16] at the Jet Propulsion Laboratory.

II. TASK ANALYSIS AND PLANNING DISPLAYS

Graphics displays can provide substantial aid in off-line task analysis and planning, for example, to investigate workcell layout, motion planning with collision detection and with possible redundancy resolution, and planning for camera images. Graphics displays are used for task analysis and planning of Solar Maximum Repair Task. The Solar Maximum Repair Mission (SMRM) [4] was successfully completed by two astronauts through a 7-hour extra vehicular activity (EVA) in 1984. In this mission, the Solar Maximum Mission (SMM) satellite was captured and berthed in the Space Shuttle cargo bay by using the Shuttle Remote Manipulator System (RMS), and then three tasks of replacing Modular Attitude Control System (MACS), installing a protective cover, and replacing the Main Electronics Box (MEB) of an instrument were performed prior to the deployment of the repaired satellite. The most difficult task among the three was the MEB repair. Central Research Laboratories (CRL) demonstrated in 1987 that the MEB repair task could be performed by teleoperation using a 7-dof force-reflecting master/slave manipulator system [1]. The same MEB repair task is planned to be demonstrated in the Advanced Teleoperation Laboratory (ATOP) by using a dual-arm teleoperation system equipped with recent advanced control and graphics display techniques. Two 8-dof redundant robot arms from AAI (American Armament Inc.) has just been installed, replacing the two existing 6-dof PUMA arms, to increase the reach volume and dexterity.

The IGRIP (Interactive Graphics Robot Instruction Program) software package from Deneb Robotics [5] is used in our initial off-line task analysis/planning of the simulated SMSR task. The package provides an excellent operator-interactive graphics simulation environment with advanced features for CAD-based model building, workcell layout, collision detection, path designation, and motion simulation.

The workcell of the simulated SMSR task shown in a graphics display of Fig. 1 consists of two 8-dof AAI robot arms, a partial SMM satellite mockup, two "smart" hands (end effectors), a raised tile floor, and a screw driver tool. Other workcell elements include camera gantry frame and

various other end effector tools such as a tape cutter to cut Kapton tapes and a diagonal cutting plier to cut tie wraps. By using CAD-based object model building functions of IGRIP, each device in the workcell was built by first creating the individual parts of the device and then putting them together with appropriate definitions of kinematic attributes. All the graphics models were built by using actual dimensions measured. After all the devices were built, these devices were laid out in the workcell by using workcell layout functions of IGRIP. Each device is allowed to be moved in any position and orientation with a mouse. In order to determine the desirable mounting locations of the robots and the satellite mockup, reach envelopes of a robot were overlaid on the workcell display graphics for various task conditions, where each device was allowed to be moved to satisfy the reach envelope constraints.

The AAI arm which has just been installed for the SMSR demonstration is an 8-dof redundant manipulator with 8 rotational joints connected serially. The axes of the first 3 joints intersect with each other at the shoulder point. Joint 4 specifies the elbow bending angle, and the first 4 joints (joint 1 through 4) determine the wrist position. The remaining 4 joints constitute a wrist, and their axes intersect with each other at the wrist point. The lengths of the upper arm (from shoulder to elbow) and the forearm (from elbow to wrist) are 27.407 in. and 21.930 in., respectively. By considering the geometry of the AAI arm, we can easily observe that the wrist reach volume which is the set of points reachable by the robot wrist point is a relatively thin spherical shell of of thickness 17.348 in. with inner and outer radii 31.989 in. and 49.337 in., respectively.

An example of the reach envelope analysis is shown in Fig. 2 to determine the opening angle of the MEB panel. Removal of electric connector screws from the MEB requires that the screw driver held by the right robot hand be able to reach all the connector screws at the right angle to the MEB panel. The total length from the wrist to the screw driver tip is 26.125 in. (screw driver tool length = 7.5 in.), and the reach envelope of the screw driver for the perpendicular orientation to the panel is obtained by translating the wrist reach envelope of Fig. 2 by 26.165 in. towards the panel. When the panel is 100° opened, some of the connector screws near the hinge assembly cannot be reached by the screw driver at the right angle (Fig. 2a). A rather long distance from the wrist to the tool tip severely restricts acceptable opening angles of the panel. Further careful reach envelope analysis indicates that when the panel is 115° opened, the screw driver can reach all the connector screws at the right angle to the panel (Fig. 2b).

An inverse kinematic routine developed for the 8-dof redundant AAI arm [14] was incorporated into each of the two graphically simulated robot arms to allow cartesian robot control. The inverse kinematic algorithm employed is a simplistic approach of fixing 2 joints and using only 6 joints at a time. At present joint 3 and 5 are chosen as fixed joints and used as redundancy control parameters. In the normal operating region of the SMSR task, the joint 3 value is

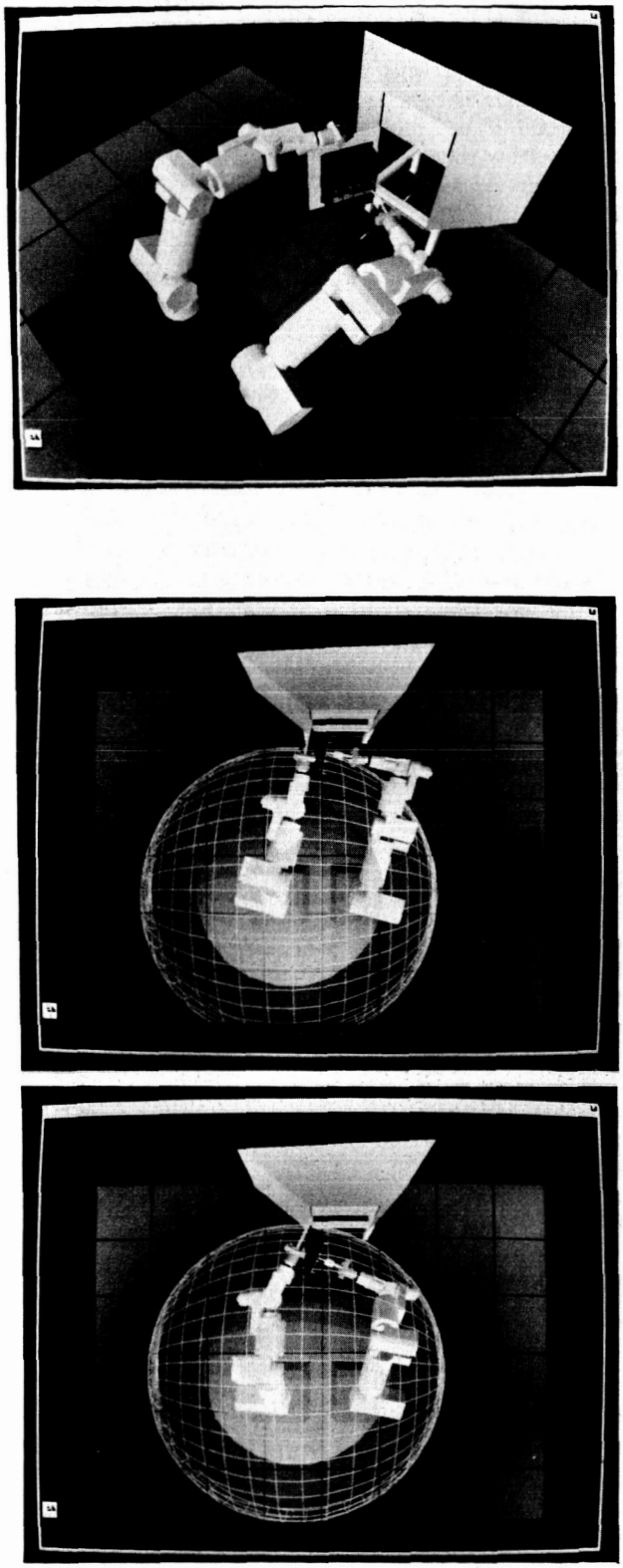

Fig. 2. The MEB panel of the satellite mockup should be inside the reach envelope of the right robot hand for folding and unfolding thermal blankets (upper) and inside the reach envelope of the tape cutter held by the right robot hand for Kapton tape cutting (lower).

closely related to the elbow rotation about the axis connecting the shoulder and wrist points. However, when the desired wrist position is right above the shoulder point, joint 3 must be 0° or 180° and in this case only joint 1 is closely related to the elbow rotation angle. The cartesian motion of each robot was verified graphically with the "T-jog" function of IGRIP. In the "T-jog" mode, the end effector frame of the robot follows the coordinate frame of a selected tag point which can be controlled with a mouse or a keyboard. The graphically simulated arms can also be controlled with hand controllers using the inverse kinematic routine residing in the real-time robot control system. This helps to check the inverse kinematic routine implemented on the real-time system.

In Fig 3, the joint 3 values of the left and right arms are inadequately set to 105° and −60°, respectively. As a result, the elbows of the two arms begin to collide with each other, as we move the right arm further away from the satellite mockup keeping the screw driver tip on the MEB surface and the orientation at the right angle to the panel. Fig. 3 shows a configuration right before collision. When the two arms collide, the collision is immediately detected by IGRIP, and the parts in collision get highlighted in red. The two arms containing the colliding parts get highlighted in cyan, and the rest of the devices in the workcell turn blue. Of course, an adequate setting of the elbow rotation angles can avoid collisions as in Fig. 1.

It cannot be overemphasized that good camera viewing conditions are essential to perform teleoperation missions successfully. Simulated graphics displays of camera views can be used for sensor planning to determine desirable camera locations and zoom settings for each task segment by using viewing criteria such as visibility, resolution, field of view, and lighting. Continuous motion simulations can be performed by using programs written in GSL (graphics simulation language) and CLI (command line interpreter) supported by IGRIP. Collisions between devices in the workcell can be detected during simulation. A final verified planned task sequence and the motion simulation for each task segment can be used later for preview display during the on-line task execution.

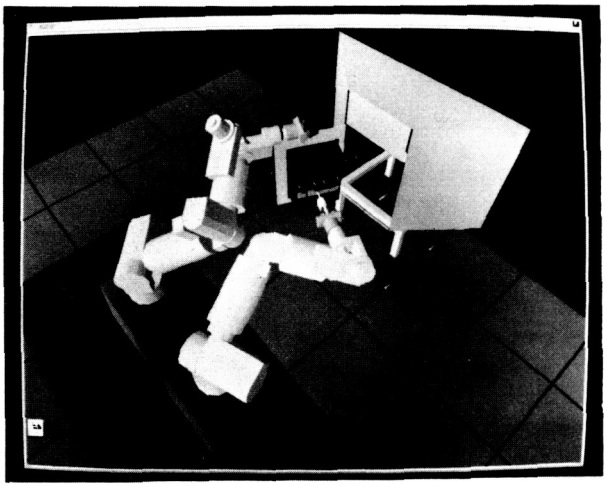

Fig. 3. Redundance resolution with the joint 3 value. An inadequate setting of the elbow rotation angle can cause collisions between the two arms.

III. OPERATOR TRAINING DISPLAYS

Graphics displays can also serve as an introductory training tool for operators. Teleoperation in general demands considerable training, and robots can be damaged during the initial stages of the training. Prior to training with actual robots, a telerobot simulator can be used during the initial training. Introductory training with a simulator can save time and cost for space crew training.

Recently we have developed a force-reflecting teleoperation simulator/trainer [7], [10], [12] as a possible computer-aided teleoperation training system (Fig. 4). A novel feature of this simulator is that the operator actually feels virtual contact forces and torques of a compliantly controlled robot hand through a force reflecting hand controller during the execution of the simulated peg-in-hole task. The simulator allows the user to specify force reflection gains and the stiffness (compliance) values of the manipulator hand for both the three translational and the three rotational axes in Cartesian space. The location of the compliance center can also be specified, although initially it is assumed to be at the grasp center of the manipulator hand.

A peg-in-hole task is used in our simulated teleoperation trainer as a generic teleoperation task. An in-depth quasi-static analysis of a two-dimensional peg-in-hole task has been reported earlier [17], but the two-dimensional model is not sufficient to be utilized in a teleoperation trainer. This two dimensional analysis is thus extended to a three-dimensional peg-in-hole task [10], [12], so that the analysis can be used in our simulated teleoperation trainer. In our three-dimensional peg-in-hole task simulation, both the hole and the peg are assumed to be cylindrical with radii of R and r, respectively (Fig. 5). Throughout the analysis, we also assume that the clearance of the hole is small, and thus the angle between the peg and hole axes is assumed to be sufficiently small, allowing small angle approximation. In general, the peg rotates and translates during execution of the peg-in-hole task, accommodating itself to the hole structure by correcting lateral and angular errors of the operator-commanded peg position and orientation. In order to have finite contact forces and torques, both lateral and angular compliance must be provided for the system. In our simulation, the hole and its support structure are assumed to be rigid with infinite stiffness, while the robot hand holding the peg is compliant for all three cartesian translational axes and also for all cartesian rotational axes (Fig. 5). We further assume that the compliance center is located at a distance L from the tip of the peg with three lateral springs k_x, k_y and k_z and three angular springs k_{mx}, k_{my}, k_{mz}. Both the operator-commanded and the actual positions of the peg are described by the position of the compliance center. No friction is assumed throughout the analysis.

For a given operator-commanded peg position, the actual peg position after compliant accommodation can be different depending upon the current state of the peg of whether the peg is currently in the hole or not. When the peg is not currently in the hole (peg-not-in-hole state), three conditions are possible: i) the peg is not in contact with the wall (no-contact condition), ii) the peg is in contact with the wall (peg-on-wall condition), and iii) the peg is in contact with the entrance of the hole. When the peg is in the hole (peg-in-hole state), four conditions are possible: i) no-contact, ii) peg-side one-point contact, iii) peg-tip one-point contact, and iv) two-point contact. In our initial development of computing virtual kinesthetic contact forces and torques, a rough approximation was used during the initial insertion transition from the peg-not-in-hole state to the peg-in-hole state. Detailed computational procedures can be found in [10], [12]. A more generalized method of computing contact forces and torques based on a general collision detection algorithm is under consideration.

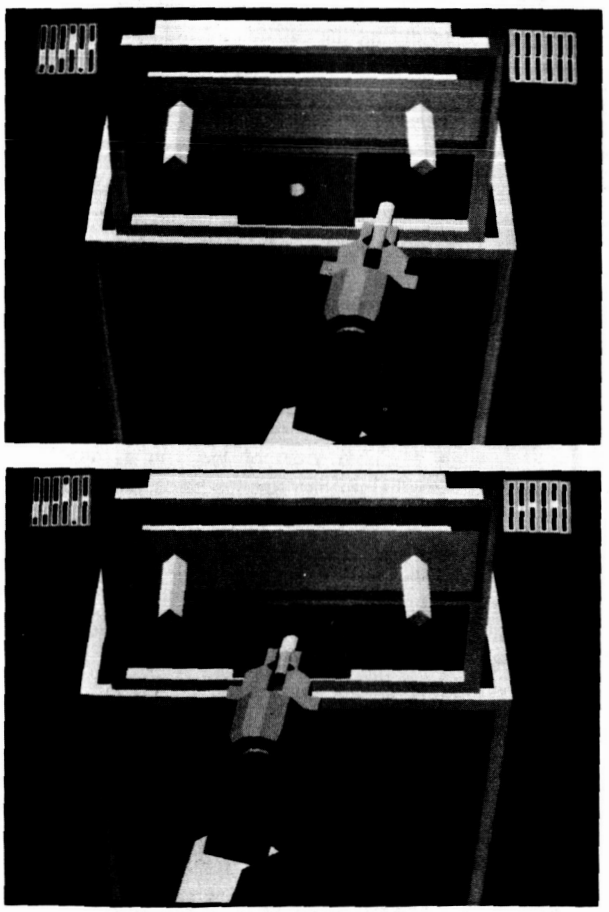

Fig. 4. Force-reflecting teleoperation training displays before contact (upper) and during insertion (lower). Contact forces and torques are computed and reflected to the force reflecting hand controller in real-time. They are also displayed on the upper left corner of the screen, while the current joint angles appear on the upper right corner.

A high fidelity real time graphics simulation of the peg-in-hole task with a PUMA arm and a generic task board has been accomplished by using a Silicon Graphics IRIS-4D/310 VGX workstation, which is very fast both in computation and in graphics rendering with hardware-supported hidden surface removal and lighting. When no contact computations are involved, the update rate of our peg-in-hole graphics simulation is as fast as the display refresh rate: 60 frames/s for workstation display and 30 frames/s for NTSC video monitor display. When force/torque computations are involved due to contact, the worst update rate is about 16 frames/s. The 6-dof hand controller motion commanded by the human operator is sent to the graphics simulation display through a serial I/O line at an about 30 Hz data update rate. Virtual contact forces and torques are computed in real time and fed back to the hand controller through the serial I/O line at an about 30 Hz data update rate. The round-trip time delay of our force-reflecting simulator system from the operator position command to the force reflection to the operator is about 30 to 80 ms.

Testings with the developed peg-in-hole task simulator/trainer indicate that appropriate compliance values are essential to achieve stable force-reflecting teleoperation in performing the simulated peg-in-hole task. As the compliance values of the simulated robot hand becomes smaller, the operator must hold the force-reflecting hand controller more firmly to maintain the stability of teleoperation. In the current implementation, robot servo system dynamics are not included.

So far we have described graphics displays for off-line task analysis/planning and simulated training. Graphics displays can also provide effective operator aid during the on-line operation. Two application examples of preview and predictive displays are described the next two sections.

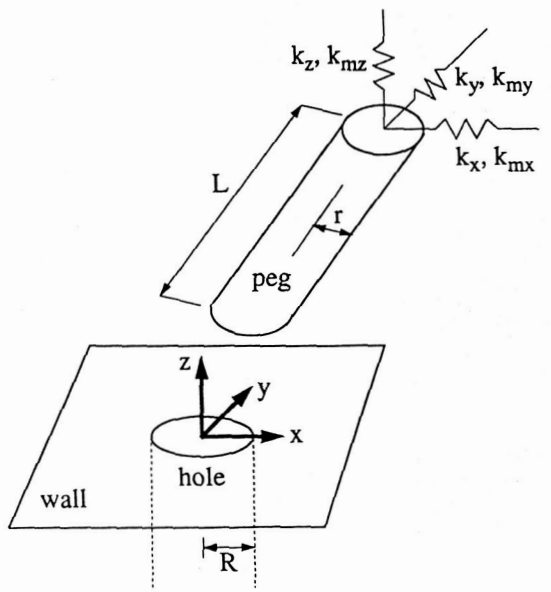

Fig. 5. Geometry of a simulated peg-in-hole task with lateral and angular springs at the compliance center.

IV. PREVIEW DISPLAYS

The success of a telerobotic space operation relies on accurate action planning and verification prior to the actual action execution. This planning/verification capability requirement becomes more significant when dual and/or redundant arm systems are operated in a constrained environment. Preview displays can provide visually perceivable and realistic action planning/verification capability for on-line task execution, thus reducing operation uncertainties and increasing operation safety.

Fig. 6 shows two examples of preview displays to be used for the SMSR operations. The operator first selects an appropriate task segment from the task segment selection menu (lower right panel). When the task segment is selected, the recommended joint angle values for joint 3 and 5 as well as the actual joint angle values are displayed with slider bar displays (upper right panel) for redundancy management. In normal operations, the operator starts with the preview mode before the task execution (upper left panel). There are four options in the preview mode: teleop, auto, record, and playback. In the preview teleop mode, the operator can rehearse the task by teleoperation using graphics simulation without sending the commands to the remote robot site. This teleop rehearsal provides the operator with opportunities not only for practice prior to task execution but also for on-line task planning such as redundancy management, collision avoidance, and sensor planning.

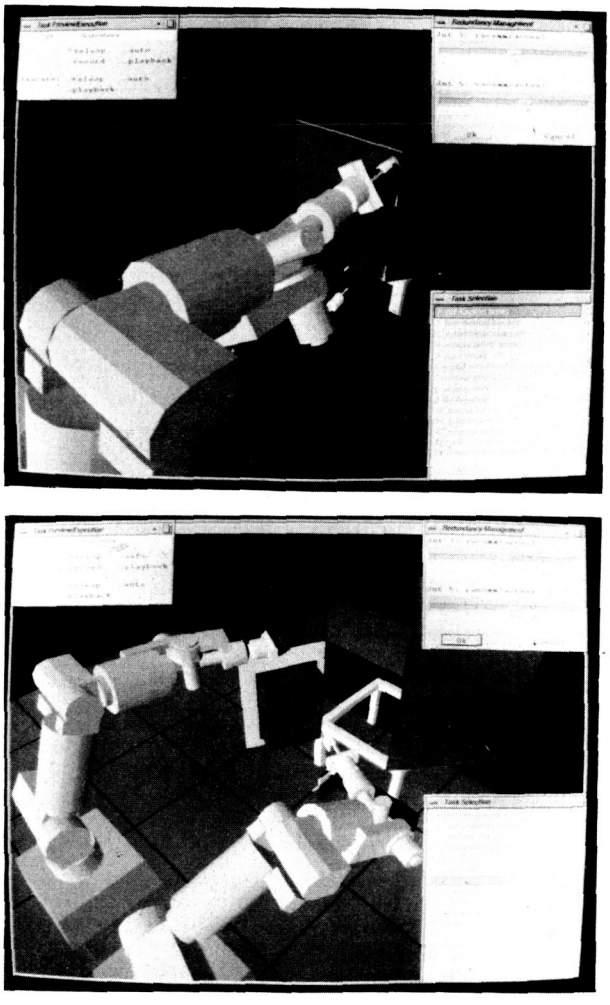

Fig. 6. Preview displays for thermal blanket tape cutting (upper) and electric connector screws removal (lower).

The operator can use the preview auto mode, if an off-line task analysis/planning was done in advance and the pre-planned task sequences are available. In this mode, the operator can see the pre-planned motion as a preview demonstration prior to the actual execution of each task segment. The preview can also record/playback options enable recording and playback of the operator's commands during the teleop rehearsal.

After the preview, the operator selects an option of the task execution mode to actual task execution. In the teleop execution mode, the operator uses manual teleoperation for task execution. In the auto execution mode, the pre-planned motion pre-stored during the off-line task analysis/planning is sent to the remote site for task execution. In the playback execution mode, the recorded motion saved during the teleop rehearsal is sent to the remote site for task execution. If the task segment requires contacts with the environment, manual teleoperation may be preferred due to the lack of accurate calibration of the task environment including cameras. However, if the task segment only needs free-space robot motion without contacts or near collisions, the automatic execution of the pre-planned robot motion may be used for efficiency. An operator intervention capability should be provided during the task execution so that the operator can stop the robot motion at any time when desired.

It is also important to note that a preview graphics display showing a global view of the arm at any desired angle can be very helpful for the operator to visualize the current arm configuration for more comfortable and safer teleoperation in both the preview and the task execution modes. During the task execution mode, the actual joint angles read from the remote robot system are sent to the local site operator control station for graphics update. In our current system, the actual robot joint angles are sent to the graphics system at a data update rate of 30 Hz through a serial I/O line. When the task environment is known, robot arm visualization can be extended to task visualization by showing the operator a graphical simulation of the entire task environment including the robot arm. Other visual cues can also be added, if desired, such as on-the-screen visual enhancements [13] or a graphical representation of a suggested redundancy resolution of a redundant arm.

V. PREDICTIVE DISPLAYS

It is in general difficult for the human operator to control a remote manipulator when the communication time delay exceeds 1 second. The best known strategy to cope with time delay is the "move and wait" strategy [6]. In this

strategy, the operator moves the manipulator a small distance and then waits to see what happens before the next move. When one wants to control a space robot from Earth, there is an unavoidable time delay in the communication link. The round-trip time delay of the communication link between the ground station and a space telerobot in low Earth orbit is expected to be 2 to 8 seconds to relay data via several communication satellites and ground stations. In order to enhance task performance in operating telemanipulators with time delay, we have recently implemented two new schemes at the Advanced Teloperation System: predictive display [2],[9] and shared compliance control [11]. Compliance control is useful during contact or insertion, while predictive display is useful during free-space motion of the the robot arm under quasi-static work environment.

In a predictive display, the graphics model responds instantaneously to the human operator's hand controller commands, while the actual camera view of the arm responds with a communication time delay. Thus the predictive display provides the operator with the non-time-delayed motion of the robot arm graphics model, while the actual robot motion occurs with delay. A predictive display system was originally developed earlier by using a stick figure model of the robot arm overlaid on the actual video image of the arm [15]. Recent advances in graphics technologies enabled us to develop a predictive display with a high-fidelity graphics model which can be either a solid-shaded or a wire-frame model. A high-fidelity graphics model of a Unimation PUMA 560 robot arm was generated and used in our predictive display. A wire-frame model with hidden line removal is sometimes advantageous compared to a solid model. When the wire-frame model of the PUMA arm is overlaid on the camera view, it does not occlude the camera view of the arm.

The real time overlay of the graphics model on the video camera image was achieved by using a video genlock board installed on a Silicon Graphics IRIS-4D/70 GT workstation. The genlock board enables the IRIS graphics output to be synchronized with the incoming video camera signal. It also provides a per-pixel video switching function. Namely, the video output of the genlock board, which is connected to the video monitor for display, can be switched to either the incoming video camera signal or the graphics output signal for each pixel, depending upon the alpha-plane value for the corresponding pixel. In our current application the 8-bit alpha-plane is used simply for graphics image overlay (superimposition), although it allows blending or mixing of two graphics images.

In order to superimpose the PUMA arm graphics model on the camera view of the actual arm, camera calibration is necessary. In our implementation (Fig. 7), camera calibration was achieved by an interactive cooperation between the human operator and the system [9]. The operator provides the correspondences between object model points and camera image points by using a mouse. Thereafter the

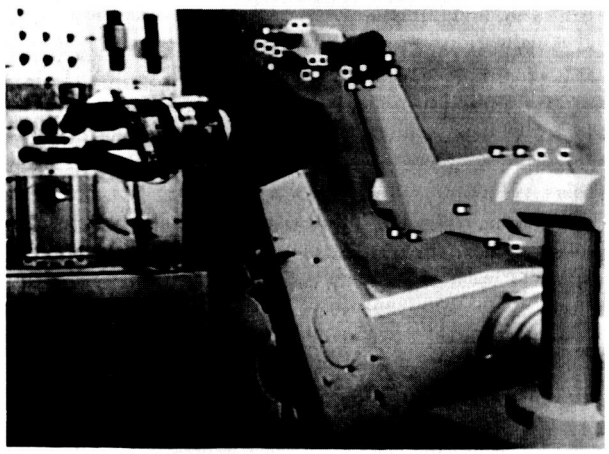

Fig. 7. Visual/manual camera calibration process for graphics overlay. Both the graphics model and the camera view of the PUMA arm appear on the screen. The human operator enters object model points and their corresponding image points using a mouse.

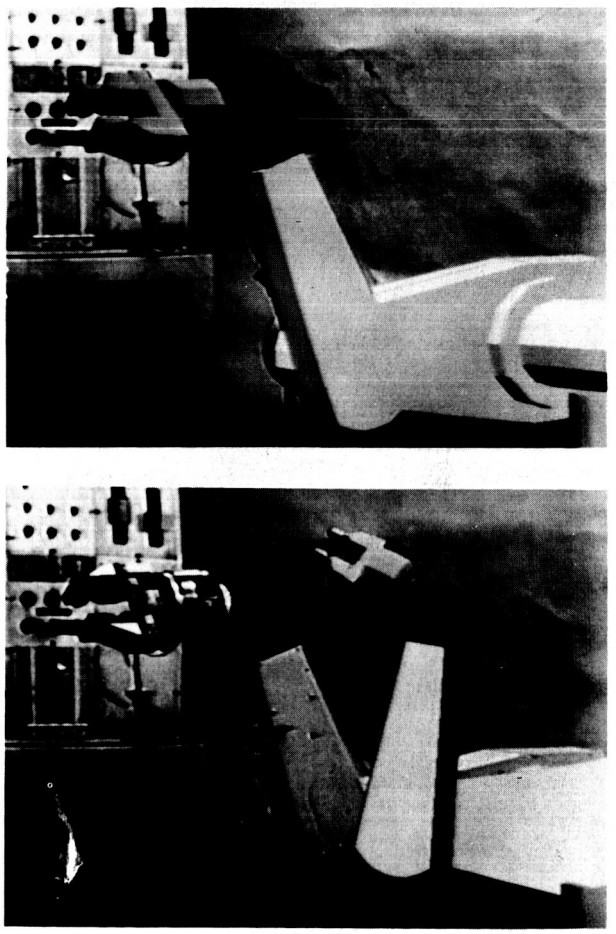

Fig. 8. Calibrated graphics overlay of the solid shaded model on the actual camera view (upper) and a snapshot of a predictive display in operating the remote arm with time delay (lower).

system computes the camera calibration matrix. A linear least-squares method can be used to determine the 12 elements of the 4×3 camera calibration matrix, when 6 or more object points and their corresponding images are given. However, the linear method does not guarantee the orthonormality of the rotation matrix. In our graphics overlay application, the orthonormalized rotation matrix may be preferred. Orthonormalization can be applied after the linear method, but this does not yield the least squares solution. In general, a nonlinear least-squares method has to be employed if we wish to obtain the nonlinear least squares solution that satisfies the orthonormality of the rotation matrix. In the nonlinear method, instead of using 9 elements of a rotation matrix, three angles (pan, tilt, swing) are used to represent the rotation. In our current design, both linear and nonlinear camera calibration algorithms are available. The algorithms above can be used for both cases of when the camera focal length f is known and unknown. The user can select any one of the camera calibration matrix solutions for rendering the PUMA arm graphics model and superimposing on the camera view.

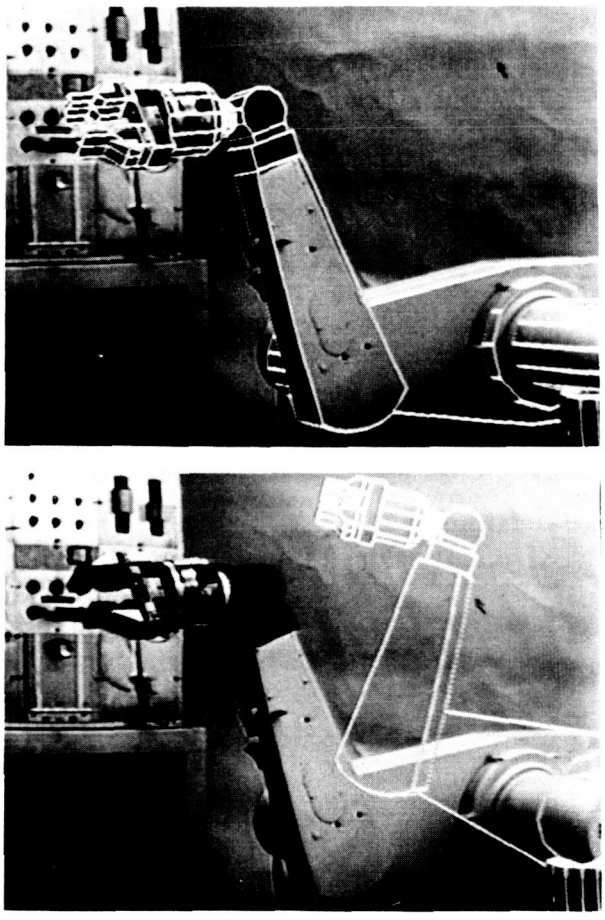

Fig. 9. Calibrated graphics overlay of the wire-frame model on the actual camera view (upper) and a snapshot of a predictive display in operating the remote arm with time delay (lower).

The PUMA arm graphics model superimposed on the actual camera view after the camera calibration is shown in Fig. 8 for the surface model and in Fig. 9 for the wire-frame model. During the actual teleoperation with a predictive display under time delay, the actual camera view of the robot arm follows the graphics model with time delay (Figs. 8b and 9b).

Preliminary experimental results with a simple single-view single-arm tapping task indicate that predictive display enhances the human operator's telemanipulation task performance significantly [2], [8], although it appears that either two-view or stereoscopic predictive displays are necessary for general 3-D tasks.

VI. FUTURE PLANS

Efficiency and reliability of space telerobotic missions will be greatly enhanced through a coherent use of graphics displays in all three phases of off-line task analysis and planning, simulated training, and on-line task execution. New developments and applications of graphics displays for each individual phase described in this paper can be utilized to attain an integrated coherent application of graphics displays throughout all three phases. At present, the simulated SMSR task is being used as a typical exemplar of a space telerobotic mission to demonstrate the effectiveness of our methodology of using graphics displays coherently in all three phases. Experiments will be performed later to quantify teleoperation performance enhancements attained through our methodology. The proposed methodology can be applied to future space telerobotics flight experiments to provide the operator with significant graphics aids during teleoperation.

VII. CONCLUSION

We described new developments and applications of graphics displays in all three phases of off-line task analysis/planning, simulated training, and on-line task execution to reduce operation uncertainties and increase operation efficiency and safety. Task analysis/planning displays provided substantial aid in investigating workcell layout, robot motion planning, and sensor planning for a simulated SMSR task. A force-reflecting training simulator with visual and kinesthetic force virtual reality was developed to serve as an introductory training tool prior to training with actual robots. On-line preview and visualization displays provide the operator with visually perceivable and realistic action planning/verification capability for on-line task execution. Predictive displays provide the operator with a non-delayed graphics model overlaid on the actual camera view to aid the human operator in operating telemanipulators with time delay. These newly developed graphics displays are currently being applied to the simulated SMSR task to demonstrate that an integrated coherent application of graphics displays in all three phases will enhance teleoperation efficiency and reliability.

ACKNOWLEDGMENT

This work was carried out at the Jet Propulsion Laboratory, California Institute of Technology, under contract with the National Aeronautic and Space Administration.

REFERENCES

[1] R. H. Adams, A. E. Gross, and C. E. Jennrich, "Remote Repair Demonstration of Solar Maximum Main Electronics Box," Central Research Laboratories, Red Wing, MN, 1987.

[2] A. K. Bejczy, and W. S. Kim, and S. Venema, "The Phantom Robot: Predictive Displays for Teleoperation with Time Delay," IEEE Int. Conf. on Robotics and Automation, pp. 546-551, Cincinnati, OH, May 1990.

[3] A. K. Bejczy, Z. Szakaly, and W. S. Kim, "A Laboratory Breadboard System for Dual-Arm Teleoperation", SOAR '89 workshop, Johnson Space Center: TX, July, 1989.

[4] F. Cepollina and J. R. Jaax, "Extra Vehicular Activity Annex: Solar Maximum Repair Mission", JSC-14082, Annex 11, NASA Johnson Space Center, Mar. 1984.

[5] Deneb Robotics Inc., IGRIP User Manual, Auburn Hills, MI, May 1991.

[6] W. R. Ferrel, "Remote Manipulation with Transmission Delay," IEEE Transactions on Human Factors in Electronics, Vol, HFE-6, Sept. 1965, pp. 24-32.

[7] W. S. Kim, "Developments of New Force Reflecting Control Schemes and an Application to a Teleoperation Training Simulator," IEEE Int. Conf. on Robotics and Automation, Nice, France, May 1992.

[8] W. S. Kim, "Experiments with a Predictive Display and Shared Compliant Control for Time-Delayed Teleoperation," IEEE Conf. on Engineering in Medicine and Biology Society, pp. 1905-1906, Philadelphia, PA, Nov. 1990.

[9] W. S. Kim, "Graphics Overlay and Camera Calibration for Predictive Displays," Jet Propulsion Laboratory Internal Document Engineering Memorandum 347-89-273, Dec. 1989.

[10] W. S. Kim and A. K. Bejczy, "Graphics Displays for Operator Aid in Telemanipulation," IEEE Conf. on Systems, Man, and Cybernetics, Charlottesville, VA, Oct. 1991.

[11] W. S. Kim, B. Hannaford, and A. K. Bejczy, "Force-Reflection and Shared Compliant Control in Operating Telemanipulators with Time Delay," IEEE Trans. on Robotics and Automation, vol. 8, no. 2, 1992.

[12] W. S. Kim and P. Schenker, "A Teloperation Training Simulator with Visual and Kinesthetic Force Virtual Reality," SPIE Conference on Human Vision, Visual Processing, and Digital Display, Society of Photo-Optical Instrumentation Engineering, San Jose, CA, Feb. 1992.

[13] W. S. Kim, F. Tendick, and L. Stark, "Visual Enhancements in Pick-and-Place Tasks: Human Operators Controlling A Simulated Cylindrical Manipulator," IEEE J. of Robotics and Automation, vol. RA-3, no. 5, pp. 418-425, 1987.

[14] S. Lee and A. K. Bejczy, "Redundant Arm Kinematics Control Based on Parameterization," IEEE Int. Conf. on Robotics and Automation, pp. 458-465, Apr. 1991.

[15] M.V. Noyes and T.B. Sheridan, "A Novel Predictor for Telemanipulation Through a Time Delay," Proc. of 20th Annual Conference on Manual Control, NASA Ames Research Center, Moffett Field, CA, 1984.

[16] P. S. Schenker, A. K. Bejczy, W. S. Kim, and S. Lee, "Advanced Man-Machine Interfaces and Control Architecture for Dextrous Teleoperations," IEEE Oceans '91, Honolulu, HI, Oct. 1991.

[17] D. E. Whitney, "Quasi-Static Assembly of Compliantly Supported Rigid Parts," J. of Dynamic Systems, Measurement, and Control, pp. 65-77, 1982.